The Torque Control with Multi-Objective Performance for E-Bike Systems with Human Power Assistance

PANG-CHIA CHEN[1], CHIH-CHING HSIAO[1,*], SUN-LI WU[1], SHYUE-BIN CHANG[2]
[1]Department of Electrical Engineering; [2]Department of Mechanical and Automation Engineering
Kao Yuan University
No.1821, Zhongshan Rd., Luzhu Dist., Kaohsiung City 821
TAIWAN, R.O.C.
t20049@cc.kyu.edu.tw , *t20051@cc.kyu.edu.tw

Abstract: -This paper proposes a velocity control approach for the light electric bike with human power assistance. The velocity control signal is composed of two signals. One is a velocity-dependent equilibratory torque to compensate the wind resistance. Another is a deviation torque to achieve desired multi-objective performance represented in terms of linear matrix inequality (LMI) conditions. The formulated multi-objective performances includes the invariant set of state variable under the magnitude bounded disturbance, the magnitude bound on the regulated output, and the $\mathcal{H}^{\infty}$ performance optimization for attenuation of various disturbance effects on the regulated output. The disturbances include the deviations of tire resistance, human assistant torque, and driver's weight from nominal values. Based on the parameters and specifications of the EL-168 electric bike produced by KENTFA Advanced Technology, Taiwan, the design results are verified through time-response simulations under both the flat and linear varying gradient road conditions.

Key-Words: - Electric Bike, Torque Control, LMI, Multi-Objective Control, Human Power Assistance

1 Introduction

According to the report by Asian Development Bank [1], the electric bike (E-Bike) gains a growing popularity especially in the People's Republic of China, starting with a modest beginning in the mid-1990s, and then over 21 million in 2007, which is almost the amount of population in Taiwan. In order to induce a shift away from the use of gasoline motorcycle, the government of Taiwan also endeavors to promote the E-Bikes' industrial and usage by providing subsidization to compensation the higher cost of E-Bike compared to a second-hand motorcycles or a simply human powered bicycle.

The E-Bike systems can be grouped at least into three categories according to their weight and rated power, in which a medium E-Bike is recognized as around a weight of 60 Kg and rated power of 450 Watt, a small E-Bike is around a weight of 40 Kg and rated power of 300 Watt [1], and the light E-Bike has about a weight of 20 Kg and rated power of 250 Watt. The scale of the light E-Bike enables the usage of human power to assist the limited electrical power capacity provided by carried battery. This flexibility will extend effectively the maneuvering scenario of the E-Bike systems. The light E-Bike also allows the alternative design to have a foldable framework, which will make the E-Bikes easy to be carrying, handling, and depositing. This approach will allow the E-Bike to be cooperatively and connectively used with the four-wheel vehicle or public transportation. In the Greater Kao-Hsiung City area of the Southern Taiwan, where is intended for application of the study in this work, the usage of the fordable light E-Bike systems is expected to complement with the Kao-Hsiung Mass Rapid Transportation systems to provide a complete, convenient, and seamless transportation network for passengers traveling.

In the research community related to the E-Bike systems control, [2-4] investigated about the dynamics derivation and the associated stability and control issues for a general single-track vehicle such as the bike. The works of [5, 6] are about autonomous control that considers steering and attitudinal stability of the E-Bikes.

This work is on the velocity control for E-Bike with both the electric torque from the motor and assistant torque from the rider. The E-Bike velocity control based on a fuzzy logic control approach was investigated in [7-9]. In [7], the authors utilized the fuzzy logic control approach to manage the supply of auxiliary electrical power with right amount on proper time to help the rider. Therefore, a satisfactory bike speed can be achieved despite the poorness of road conditions and defectiveness of

rider's physical condition. In [8], the fuzzy logic controlled electric hybrid bike was investigated with emphasis on energy efficiency. The design and simulation analysis are presented. The work of [9] was on the physical realization of the automatic E-bikes speed control based on fuzzy logic and programmable system-on-chips approach.

The studies in [10, 11] inspected the effect of human assistant torque from the rider. In [10], the human input and running friction are estimated as a disturbance torque. Thee human input is separated from the running friction by using a high pass filter; thereafter, a disturbance observer was used to estimate the running friction. The proposed scheme of power assistance then can be implemented without torque sensor. In the work of [11], the human torque input was decomposed into two parts, including the constant average torque and the fluctuating torque. The repetitive control approach was used for improving the comfort of rider in the uphill riding condition.

In the refs of [12,13] for E-Bike velocity control were proposed in an optimization basis in terms of $\mathcal{H}^{\infty}$ performance. In [12], the design of the robust controller was considered as a speed-current dual-loop system. Both simulations and experiments were conducted. The work in [13] formulated the velocity/energy control problem in terms of optimization of disturbance attenuation performance. Two performance indexes regarding the quickness and economics were addressed and tuned to meet various requirements for controller design. The controller was constructed numerically via the convex linear matrix inequality (LMI) approach [14].

For this study of velocity control for E-Bike, the torque control law comprises two parts; one is a velocity-dependent control signal to maintain vehicle's equilibratory operation condition, another is the deviation control signal obtained from optimal control method to achieve multi-objective performances regarding the external disturbance input, control signal magnitude, and velocity tracking error. The optimal control signal is designed in terms of LMI conditions [14]. The addressed objective performance includes: (1) the invariant set of state variable under the magnitude bounded disturbance, which include the uncertainties of human torque, tire resistance, gradient resistance, and the magnitude of velocity tracking command, (2) the magnitude bound on the regulated output including the tracking error and control magnitude, and (3) the $\mathcal{H}^{\infty}$ performance optimization from the disturbance to the regulated output.

The remains of this paper are organized as follows. Section 2 presents the modeling of the E-Bike systems, including the vehicle kinematics, various resistances, and specifications of the named EL-168 E-Bike produced by KENTFA Advanced Technology, Taiwan. Also, the derivation of the velocity-dependent control law to compensate for the wind resistance is given. In Section 3, the optimal control structure is formulated and the individual performance condition is derived in terms of the LMIs. Then, Section 4 is the numerical synthesis for the optimal control law under the given vehicle parameters and specifications. The time response simulation of the closed-loop controlled system is conducted based the proposed control approach, which composes of both the velocity-dependent equilibrator control signal and the multi-objective optimal deviation control signal. Finally, Section 5 is the conclusion.

2 Modeling and Velocity-Dependent Control Law

2.1 Vehicle Kinematics

The motion of E-Bike vehicle can be described by [7],

$$I\ddot{\theta} = \tau_{\mathrm{m}} + \tau_{\mathrm{b}} - \tau_{\mathrm{w}} - \tau_{\mathrm{r}} - \tau_{\alpha}, \tag{1}$$

where I denotes the moment of inertia; θ denotes the angle of wheel; τ_{m} denotes the human torque; τ_{b} denotes the torque from battery; τ_{w} denotes the wind resistance torque; τ_{r} denotes the tire resistance torque; τ_{α} denoted the gradient resistance torque. By the equality relating the vehicle velocity, tire radius, and angular velocity, $v = r\dot{\theta}$, (1) can be rewritten as,

$$\left(\frac{I}{r}\right)\dot{v} = \tau_{\mathrm{m}} + \tau_{\mathrm{b}} - \tau_{\mathrm{w}} - \tau_{\mathrm{r}} - \tau_{\mathrm{d}}. \tag{2}$$

2.2 Various Resistances

The resistances of vehicle during operation include the sources from the wind, the rolling tire, and the gradient angle of road. The wind resistance force and torque can be represented as,

$$F_{\mathrm{w}} = C_{\mathrm{w}}\frac{\gamma}{2g}v^2 A, \tag{3}$$

$$\tau_{\mathrm{w}} = F_{\mathrm{w}} r_e \cong F_{\mathrm{w}} r = C_{\mathrm{w}} \frac{\gamma}{2g} v^2 A r, \qquad (4)$$

where $C_{\mathrm{w}} = 1.8$ is the wind resistance coefficient; $\gamma = 1.293\,(\mathrm{Kg/m^3})$is the air density; $g = 9.8\,(\mathrm{m/sec^2})$ is the gravitational acceleration; $A = 0.35\,(\mathrm{m^2})$ is the vehicle frontal area; and $r_e \cong r = 0.1524\,(\mathrm{m})$ is the actual tire radius during motion.

The resistance of tire consists of two parts, one is due to the contact friction between the tire and the road surface, and another is from the required rolling torque under vehicle weight and deformation of tire. The contact friction coefficient for a usual road surface is reported as 0.01~0.015 from the Cycling & Health R&D Center, Taiwan. In this study, the quantity of this friction is adopted as, $f_{\mathrm{r,c}} \cong 0.012$. The rolling resistance coefficient is defined and can be approximately computed as,

$$f_{\mathrm{r,t}} \triangleq \frac{\tau_{\mathrm{r,t}}}{Wr} \cong \frac{\tau_{\mathrm{r,t}}}{W_{\mathrm{z}} r_{\mathrm{e}}} = \frac{W_{\mathrm{z}} r_{\mathrm{r}}}{W_{\mathrm{z}} r_{\mathrm{e}}} = \frac{r_{\mathrm{r}}}{r_{\mathrm{e}}} \qquad (5)$$

with $r_{\mathrm{e}} = v/\omega$. The corresponding rolling resistance torque is,

$$\tau_{\mathrm{r,t}} = W_{\mathrm{z}} r_{\mathrm{e}} f_{\mathrm{r,t}} = W r f_{\mathrm{r,t}} \cong W r_{\mathrm{r}} \qquad (6)$$

For the reaction rolling radius of tire, r_{r}, in (5) and (6), from the definition of tire pressure, we can have the identity, $2 r_{\mathrm{r}} w_{\mathrm{r}} P_{\mathrm{r}} = W$; therefore, the rolling resistance coefficient in (5) can be obtained as,

$$f_{\mathrm{r,t}} = \frac{r_{\mathrm{r}}}{r_{\mathrm{e}}} = \frac{1}{2 w_{\mathrm{r}} r_{\mathrm{e}}} \frac{W}{P_{\mathrm{r}}} \qquad (7)$$

The total rolling resistance torque can be computed as,

$$\tau_{\mathrm{r}} = W r \left(f_{\mathrm{r,c}} + f_{\mathrm{r,t}} \right) \cong W r \left(0.012 + \frac{W}{2 w_{\mathrm{r}} r_{\mathrm{e}} P_{\mathrm{r}}} \right) \qquad (8)$$

The gradient resistance force is $F_\alpha = W \sin\alpha$ and the gradient resistance torque is,

$$\tau_\alpha = F_\alpha r = W \sin\alpha r \qquad (9)$$

2.3 Parameters and Specifications of Motor

The functions of electric motor certainly play a central role in an E-Bike system. In this study, the parameters of motor are derived from the specifications of the E-Bike produced by KENTFA Advanced Technology, Taiwan. For the E-Bike numbered as EL-168, the wheel is of 12 inch size, the gross weight is 21 Kg, and the maximum weight for rider is 100 Kg. This E-Bike is equipped with a hub type motor, which consumes a rated power input 290 Watt and produces an expected power output 250 Watt at a rated velocity 20 Km/hr. The torque of motor at the rated power and velocity can be computed as,

$$\begin{aligned} \tau_{\mathrm{b,rate}} &= \frac{p_{\mathrm{rate}}}{\dot{\theta}_{\mathrm{rate}}} = \frac{p_{\mathrm{rate}} r}{v_{\mathrm{rate}}} = \frac{p_{\mathrm{rate}} r}{v_{\mathrm{rate,km}} / 3.6} \\ &= \frac{250 \times 0.1524}{20 / 3.6} \\ &\cong 6.8580\,(\mathrm{Nt\text{-}m}) = 0.6998\,(\mathrm{Kg\text{-}m}) \end{aligned}$$

2.4 Velocity-Dependent Control Law

The wind resistance can be obtained from (4) as, $\tau_{\mathrm{w}} = 0.042 v^2$. For the considered vehicle weight, $W \in [40, 80, 120]$, the corresponding tire resistance can be computed from (5) as, $\tau_{\mathrm{r}} = [0.2886, 1.0080, 2.1583]$. Let the tire resistance denoted as, $\tau_{\mathrm{r}} := \tau_{\mathrm{r,0}} + \delta\tau_{\mathrm{r}}$, with nominal tire resistance, $\tau_{\mathrm{r,0}} = 1.0080$, computed for $W = 80$. The possible bound on deviation of tire resistance is,

$$\begin{aligned} |\delta\tau_r| &\le \max\{|0.2886 - 1.0080|, |2.1583 - 1.0080|\} \\ &= 1.1503 := \Delta\tau_{\mathrm{r}}. \end{aligned}$$

For the rational gradient angle, $\alpha \in [-10^{\mathrm{o}}, 10^{\mathrm{o}}]$, the resistant force is represented as, $W_\alpha = W_{\alpha 0} + \delta W_\alpha$, where $W_{\alpha 0} = 0$, $\delta W_\alpha = W \sin\alpha$. For the maximum considered vehicle weight $W_{\max} = 120$, the possible bound on deviation of gradient force and torque are obtained as,

$|\delta W_\alpha| \le W_{\max} \sin\alpha_{\max} = 120 \sin 10^{\mathrm{o}} = 20.8738 := \Delta W_\alpha$, and $|r\delta W_\alpha| \le r\Delta W_\alpha = 3.1812 := \Delta\tau_\alpha$, respectively. Also, let the human torque is represented as, $\tau_{\mathrm{m}} = \tau_{\mathrm{m0}} + \delta\tau_{\mathrm{m}}$, with the bound on deviation of human torque, $|\delta\tau_{\mathrm{m}}| \le \tau_{\mathrm{b,max}} := \Delta\tau_{\mathrm{m}}$. In this study, the human torque uncertain bound is assumed equivalent to the motor rated torque, $\Delta\tau_{\mathrm{m}} = \tau_{\mathrm{e,rate}} = 0.6998\,(\mathrm{Kg\text{-}m})$.

From the vehicle kinematical modeling (1), the equilibrium torque from motor for maintaining a steady-state velocity is obtained from the addressed various resistances as,

$$\tau_{\mathrm{b}} = 0.042v^2 + (\tau_{\mathrm{r},0} + \delta\tau_{\mathrm{r}}) + r\delta W_{\alpha} - (\tau_{\mathrm{m}0} + \delta\tau_{\mathrm{m}}).$$

Disregarding the uncertainties on resistances and human torque, the equilibrium torque with velocity dependence is computed as,

$$\tau_{\mathrm{b,e}} = 0.042v^2 + \tau_{\mathrm{r},0} \tag{10}$$

Let the motor electrical torque be represented as,

$$\tau_{\mathrm{b}} := \tau_{\mathrm{b,e}} + \tau_{\mathrm{b,c}} \tag{11}$$

and substituted into (1), the vehicle kinematics model with the electrical torque $\tau_{\mathrm{b,c}}$ as control input, can be revised as,

$$\dot{v} = \frac{r}{I}\left(\delta\tau_{\mathrm{m}} - \delta\tau_{\mathrm{r}} - r\delta W_{\alpha}\right) + \frac{r}{I}\tau_{\mathrm{b,c}}, \tag{12}$$

which is illustrated in Fig. 1. The manipulated motor electrical torque τ_{b} in (11) is composed of the velocity-dependent torque $\tau_{\mathrm{b,e}}$ from (10) for vehicle equilibratory operation, and the deviated torque $\tau_{\mathrm{b,c}}$ from the following optimal controller design based on LMIs for addressing the various uncertain disturbances imposed on the vehicle, including $\{\delta\tau_{\mathrm{m}}, \delta\tau_{\mathrm{r}}, r\delta W_{\alpha}\}$.

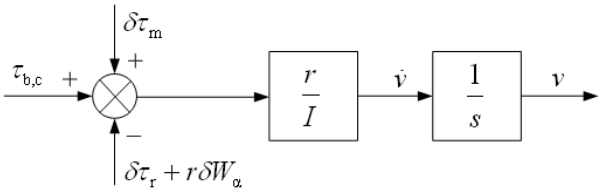

Fig. 1 Block diagram of E-Bike dynamics

3 Multi-Objective Optimal Controller Design

3.1 Formulation of Optimal Controller Synthesis

To Proceed the optimal controller design for the control torque, $\tau_{\mathrm{b,c}}$, denoting v_{d}, the velocity command and v, the actual velocity, let the vehicle states possess the velocity tracking error, $\bar{v} := v - v_{\mathrm{d}}$, and the introduced extra integrated tracking error, $e_{\mathrm{i}} := \int(-\bar{v})\,d\tau = \int(v_{\mathrm{d}} - v)\,d\tau.$ Let the velocity tracking error and the control torque are the signals to be regulated, that is, $z_{\mathrm{e}} = v_{\mathrm{d}} - v,\ z_{\mathrm{u}} = \tau_{\mathrm{b,c}}$. With the following denotations for system state $\mathbf{x}$, control u , disturbance $\mathbf{d}$, and regulated output $\mathbf{z}$,

$$\begin{aligned} &\mathbf{x} := \begin{pmatrix} \bar{v} & e_{\mathrm{i}} \end{pmatrix}^{\mathrm{T}},\ u := \tau_{\mathrm{b,c}}, \\ &\mathbf{d} = \begin{pmatrix} \delta\tau_{\mathrm{m}} & \delta\tau_{\mathrm{r}} & r\delta W_{\alpha} & v_{\mathrm{d}} \end{pmatrix}^{\mathrm{T}}, \\ &\mathbf{z} = \begin{pmatrix} z_{\mathrm{e}} & z_{\mathrm{u}} \end{pmatrix}^{\mathrm{T}} \end{aligned} \tag{13}$$

The system can be represented as the standard controller synthesis formulation,

$$\begin{cases} \dot{\mathbf{x}} = \mathbf{A}\mathbf{x} + \mathbf{B}_{\mathrm{d}}\mathbf{d} + \mathbf{B}_{\mathrm{u}}u \\ \mathbf{z} = \mathbf{C}_{z}\mathbf{x} + \mathbf{D}_{\mathrm{d}}\mathbf{d} + \mathbf{D}_{\mathrm{u}}u \end{cases} \tag{14}$$

where

$$\mathbf{A} = \begin{bmatrix} 0 & 0 \\ -1 & 0 \end{bmatrix},\ \mathbf{B}_{\mathrm{d}} = \begin{bmatrix} \frac{r}{I} & \frac{-r}{I} & \frac{-r}{I} & 0 \\ 0 & 0 & 0 & 1 \end{bmatrix},\ \mathbf{B}_{\mathrm{u}} = \begin{bmatrix} \frac{r}{I} \\ 0 \end{bmatrix}$$

$$\mathbf{C}_{z} = \begin{bmatrix} -1 & 0 \\ 0 & 0 \end{bmatrix},\ \mathbf{D}_{\mathrm{d}} = \begin{bmatrix} 0 & 0 & 0 & 1 \\ 0 & 0 & 0 & 0 \end{bmatrix},\ \mathbf{D}_{\mathrm{u}} = \begin{bmatrix} 0 \\ 1 \end{bmatrix}$$

After the synthesized state-feedback control law, $u = \mathbf{k}\mathbf{x},$ the closed-loop system becomes,

$$\begin{cases} \dot{\mathbf{x}} = \left(\mathbf{A} + \mathbf{B}_{\mathrm{u}}\mathbf{k}\right)\mathbf{x} + \mathbf{B}_{\mathrm{d}}\mathbf{d} \\ \mathbf{z} = \left(\mathbf{C}_{z} + \mathbf{D}_{\mathrm{u}}\mathbf{k}\right)\mathbf{x} + \mathbf{D}_{\mathrm{d}}\mathbf{d} \end{cases} \tag{15}$$

The multi-objective optimal controller is constructed via LMIs constraints and derived based on the assumption of a quadratic Lyapunov function,

$$V = \mathbf{x}^{\mathrm{T}}\mathbf{P}\mathbf{x},\ \ \mathbf{P} > 0 \tag{16}$$

The multi-objective performance includes the invariant set on state variables under the magnitude bounded disturbance, the magnitude constraints on the regulated output, and the $\mathcal{H}^{\infty}$ performance related the regulated output to the disturbance input.

3.2 Invariant Set under Magnitude Bounded Disturbance

The time derivative of the Lyapunov function in (16) along the trajectory of vehicle dynamics defined in (14) can be written as,

$$\begin{aligned} \dot{V} = \mathbf{x}^{\mathrm{T}}&\left[\left(\mathbf{A} + \mathbf{B}_{\mathrm{u}}\mathbf{k}\right)^{\mathrm{T}}\mathbf{P} + \mathbf{P}\left(\mathbf{A} + \mathbf{B}_{\mathrm{u}}\mathbf{k}\right)\right]\mathbf{x} \\ &+ \mathbf{x}^{\mathrm{T}}\mathbf{P}\mathbf{B}_{\mathrm{d}}\mathbf{d} + \mathbf{d}^{\mathrm{T}}\mathbf{B}_{\mathrm{d}}^{\mathrm{T}}\mathbf{P}\mathbf{x} \end{aligned} \tag{17}$$

By the fact,

$$\mathbf{x}^{\mathrm{T}}\mathbf{P}\mathbf{B}_{\mathrm{d}}\mathbf{d}+\mathbf{d}^{\mathrm{T}}\mathbf{B}_{\mathrm{d}}^{\mathrm{T}}\mathbf{P}\mathbf{x}\le\frac{1}{\eta}\mathbf{x}^{\mathrm{T}}\mathbf{P}\mathbf{B}_{\mathrm{d}}\mathbf{B}_{\mathrm{d}}^{\mathrm{T}}\mathbf{P}\mathbf{x}+\eta\mathbf{d}^{\mathrm{T}}\mathbf{d},\ \eta>0,$$

The derivative of Lyapunov function in (17) satisfies the inequality,

$$\dot{V}\le\mathbf{x}^{\mathrm{T}}\left[\left(\mathbf{A}+\mathbf{B}_{\mathrm{u}}\mathbf{k}\right)^{\mathrm{T}}\mathbf{P}+\mathbf{P}\left(\mathbf{A}+\mathbf{B}_{\mathrm{u}}\mathbf{k}\right)+\frac{1}{\eta}\mathbf{P}\mathbf{B}_{\mathrm{d}}\mathbf{B}_{\mathrm{d}}^{\mathrm{T}}\mathbf{P}\right]\mathbf{x}+\eta\mathbf{d}^{\mathrm{T}}\mathbf{d}$$

According to the discussion in Section 2.4, the quadratic term of disturbance is bounded by the magnitude constraint,

$$\mathbf{d}^{\mathrm{T}}\mathbf{d}\le\Delta\tau_{\mathrm{m}}^{2}+\Delta\tau_{\mathrm{r}}^{2}+r^{2}\Delta W_{\alpha}^{2}+v_{\mathrm{d,max}}^{2}:=\mathbf{d}_{\max}^{\mathrm{T}}\mathbf{d}_{\max}=13.8620.$$

By denoting,

$$J:=\left(\mathbf{A}+\mathbf{B}_{\mathrm{u}}\mathbf{k}\right)^{\mathrm{T}}\mathbf{P}+\mathbf{P}\left(\mathbf{A}+\mathbf{B}_{\mathrm{u}}\mathbf{k}\right)+\frac{1}{\eta}\mathbf{P}\mathbf{B}_{\mathrm{d}}\mathbf{B}_{\mathrm{d}}^{\mathrm{T}}\mathbf{P},$$

if the following inequality is true,

$$J+\eta\mathbf{P}\mathbf{d}_{\max}^{\mathrm{T}}\mathbf{d}_{\max}<0 \tag{18}$$

then the derivative of Lyapunov function satisfies,

$$\dot{V}<-\mathbf{x}^{\mathrm{T}}\left[\eta\mathbf{P}\mathbf{d}_{\max}^{\mathrm{T}}\mathbf{d}_{\max}\right]\mathbf{x}+\eta\mathbf{d}_{\max}^{\mathrm{T}}\mathbf{d}_{\max}. \tag{19}$$

From (19), we have $\dot{V}<0$, for $\mathbf{x}^{\mathrm{T}}\mathbf{P}\mathbf{x}=1$, that is, by the state-feedback control law, the state variables can always be restricted to the ellipsoidal invariant set,

$$\mathbf{x}^{\mathrm{T}}\mathbf{P}\mathbf{x}\le 1. \tag{20}$$

By using Schur's complement [14], the desired inequality (18) is written as,

$$\begin{pmatrix}\left(\mathbf{A}+\mathbf{B}_{u}\mathbf{k}\right)^{\mathrm{T}}\mathbf{P}+\mathbf{P}\left(\mathbf{A}+\mathbf{B}_{u}\mathbf{k}\right)+\eta\mathbf{P}\mathbf{d}_{\max}^{\mathrm{T}}\mathbf{d}_{\max} & \mathbf{P}\mathbf{B}_{\mathrm{d}}\\ \mathbf{B}_{\mathrm{d}}^{\mathrm{T}}\mathbf{P} & -\eta\mathbf{I}\end{pmatrix}<0 \tag{21}$$

By denoting $\mathbf{Q}:=\mathbf{P}^{-1}$, pre- and post-multiplying, $\mathrm{diag}(\mathbf{Q},\mathbf{I})$, (21) can be rewritten as the following LMI condition,

$$\mathcal{L}_{\mathrm{invar}}:=\begin{pmatrix}\mathbf{Q}\mathbf{A}^{\mathrm{T}}+\mathbf{g}^{\mathrm{T}}\mathbf{B}_{\mathrm{u}}^{\mathrm{T}}+\mathbf{A}\mathbf{Q}+\mathbf{B}_{\mathrm{u}}\mathbf{g}+\eta\mathbf{Q}\mathbf{d}_{\max}^{\mathrm{T}}\mathbf{d}_{\max} & \mathbf{B}_{\mathrm{d}}\\ \mathbf{B}_{\mathrm{d}}^{\mathrm{T}} & -\eta\mathbf{I}\end{pmatrix}<0 \tag{22}$$

where the synthesis variables, $\mathbf{g}:=\mathbf{k}\mathbf{Q},\ \mathbf{Q}>0,\ \eta>0.$

3.3 Magnitude Constraints on Regulated Output

If the regulated output defined in (13) is subject to magnitude constraints, $\mathbf{z}_{\mathrm{i}}\le\mathbf{z}_{\mathrm{i,max}}$, that is,

$$\left[\left(\mathbf{C}_{z}+\mathbf{D}_{\mathrm{u}}\mathbf{k}\right)\mathbf{x}+\mathbf{D}_{\mathrm{d}}\mathbf{d}\right]_{\mathrm{i}}\le\mathbf{z}_{\mathrm{i,max}} \tag{23}$$

By the fact,

$$\left[\left(\mathbf{C}_{z}+\mathbf{D}_{\mathrm{u}}\mathbf{k}\right)\mathbf{x}+\mathbf{D}_{\mathrm{d}}\mathbf{d}\right]^{\mathrm{T}}\left[\left(\mathbf{C}_{z}+\mathbf{D}_{\mathrm{u}}\mathbf{k}\right)\mathbf{x}+\mathbf{D}_{\mathrm{d}}\mathbf{d}\right]\le\mathbf{x}^{\mathrm{T}}\left[\left(1+\frac{1}{\eta_{\mathrm{d}}}\right)\left(\mathbf{C}_{z}+\mathbf{D}_{\mathrm{u}}\mathbf{k}\right)^{\mathrm{T}}\left(\mathbf{C}_{z}+\mathbf{D}_{\mathrm{u}}\mathbf{k}\right)\right]\mathbf{x}+\left(1+\eta_{\mathrm{d}}\right)\mathbf{d}^{\mathrm{T}}\mathbf{D}_{\mathrm{d}}^{\mathrm{T}}\mathbf{D}_{\mathrm{d}}\mathbf{d},\ \eta_{\mathrm{d}}>0$$

The magnitude constraints in (23) can be sufficiently established by,

$$\mathbf{x}^{\mathrm{T}}\left[\left(1+\frac{1}{\eta_{\mathrm{d,i}}}\right)\left(\mathbf{C}_{z}+\mathbf{D}_{\mathrm{u}}\mathbf{k}\right)_{\mathrm{i}}^{\mathrm{T}}\left(\mathbf{C}_{z}+\mathbf{D}_{\mathrm{u}}\mathbf{k}\right)_{\mathrm{i}}\right]\mathbf{x}+\left(1+\eta_{\mathrm{d,i}}\right)\left(\mathbf{D}_{\mathrm{d}}\mathbf{d}\right)_{\mathrm{i}}^{\mathrm{T}}\left(\mathbf{D}_{\mathrm{d}}\mathbf{d}\right)_{\mathrm{i}}\le\mathbf{z}_{\mathrm{i,max}}^{2},$$

and can be rewritten as the following from (20),

$$\mathbf{x}^{\mathrm{T}}\left[\left(1+\frac{1}{\eta_{\mathrm{d,i}}}\right)\left(\mathbf{C}_{z}+\mathbf{D}_{\mathrm{u}}\mathbf{k}\right)_{\mathrm{i}}^{\mathrm{T}}\left(\mathbf{C}_{z}+\mathbf{D}_{\mathrm{u}}\mathbf{k}\right)_{\mathrm{i}}\right]\mathbf{x}\le\left(\mathbf{z}_{\mathrm{i,max}}^{2}-\left(1+\eta_{\mathrm{d,i}}\right)\left(\mathbf{D}_{\mathrm{d}}\mathbf{d}\right)_{\mathrm{i}}^{\mathrm{T}}\left(\mathbf{D}_{\mathrm{d}}\mathbf{d}\right)_{\mathrm{i}}\right)\mathbf{x}^{\mathrm{T}}\mathbf{P}\mathbf{x},$$

which is equivalent to the following matrix inequality,

$$\left(1+\frac{1}{\eta_{\mathrm{d,i}}}\right)\left(\mathbf{C}_{z}+\mathbf{D}_{\mathrm{u}}\mathbf{k}\right)_{\mathrm{i}}^{\mathrm{T}}\left(\mathbf{C}_{z}+\mathbf{D}_{\mathrm{u}}\mathbf{k}\right)_{\mathrm{i}}-\left(\mathbf{z}_{\mathrm{i,max}}^{2}-\left(1+\eta_{\mathrm{d,i}}\right)\left(\mathbf{D}_{\mathrm{d}}\mathbf{d}\right)_{\mathrm{i}}^{\mathrm{T}}\left(\mathbf{D}_{\mathrm{d}}\mathbf{d}\right)_{\mathrm{i}}\right)\mathbf{P}\le 0$$

and rewritten as,

$$\begin{pmatrix}\left[\left(1+\eta_{\mathrm{d,i}}\right)\left(\mathbf{D}_{\mathrm{d}}\mathbf{d}\right)_{\mathrm{i}}^{\mathrm{T}}\left(\mathbf{D}_{\mathrm{d}}\mathbf{d}\right)_{\mathrm{i}}-\mathbf{z}_{\mathrm{i,max}}^{2}\right]\mathbf{P} & (*)^{\mathrm{T}} & (*)^{\mathrm{T}}\\ \left(\mathbf{C}_{z}+\mathbf{D}_{\mathrm{u}}\mathbf{k}\right)_{\mathrm{i}} & -1 & (*)^{\mathrm{T}}\\ \left(\mathbf{C}_{z}+\mathbf{D}_{\mathrm{u}}\mathbf{k}\right)_{\mathrm{i}} & 0 & -\eta_{\mathrm{d,i}}\end{pmatrix}<0, \tag{24}$$

where "*" is denoted for symmetric matrix components.

By pre- and post-multiplying, diag$(\mathbf{Q,I,I})$, (24) can be represented as the following LMI constraint in terms of the synthesis variables, $\mathbf{g} := \mathbf{kQ},\ \mathbf{Q} > 0,\ \eta_{\mathrm{d,i}} > 0$,

$$\mathcal{L}_{\mathrm{reg,i}} := \begin{pmatrix} \left[\left(1+\eta_{\mathrm{d,i}}\right)\left(\mathbf{D}_{\mathrm{d}}\mathbf{d}\right)_{\mathrm{i}}^{\mathrm{T}}\left(\mathbf{D}_{\mathrm{d}}\mathbf{d}\right)_{\mathrm{i}} - \mathbf{z}_{\mathrm{i,max}}^2\right]\mathbf{Q} & (*)^{\mathrm{T}} & (*)^{\mathrm{T}} \\ \left(\mathbf{C}_z\mathbf{Q}+\mathbf{D}_{\mathrm{u}}\mathbf{g}\right)_{\mathrm{i}} & -1 & (*)^{\mathrm{T}} \\ \left(\mathbf{C}_z\mathbf{Q}+\mathbf{D}_{\mathrm{u}}\mathbf{g}\right)_{\mathrm{i}} & 0 & -\eta_{\mathrm{d,i}} \end{pmatrix} < 0 \tag{25}$$

3.4 $\mathcal{H}^\infty$ Performance Optimization

The $\mathcal{H}^\infty$ performance is defined as the energy norm between the regulated output and the disturbance input, denoted as,

$$\left\|H(s)\right\|_\infty = \left(\frac{\int_0^\infty \mathbf{z}^{\mathrm{T}}\mathbf{z}dt}{\int_0^\infty \mathbf{d}^{\mathrm{T}}\mathbf{d}dt}\right)^{1/2} \le \gamma.$$

The achieved performance level γ can also be expressed as, $\int_0^\infty \mathbf{z}^{\mathrm{T}}\mathbf{z}dt \le \gamma^2 \int_0^\infty \mathbf{d}^{\mathrm{T}}\mathbf{d}dt$, or equivalently written as,

$$\int_0^\infty \left(\gamma^{-1}\mathbf{z}^{\mathrm{T}}\mathbf{z} - \gamma\mathbf{d}^{\mathrm{T}}\mathbf{d}\right)dt \le 0. \tag{26}$$

Define,

$\Gamma(k) = \int_0^k \left(\gamma^{-1}\mathbf{z}^{\mathrm{T}}\mathbf{z} - \gamma\mathbf{d}^{\mathrm{T}}\mathbf{d} + \dot{V}\right)dt - \left(V(k) - V(0)\right)$,

then for zero initial condition $V(0)$, we have,

$$\Gamma(k) = \int_0^k \left(\gamma^{-1}\mathbf{z}^{\mathrm{T}}\mathbf{z} - \gamma\mathbf{d}^{\mathrm{T}}\mathbf{d} + \dot{V}\right)dt - V(k)$$
$$\le \int_0^k \left(\gamma^{-1}\mathbf{z}^{\mathrm{T}}\mathbf{z} - \gamma\mathbf{d}^{\mathrm{T}}\mathbf{d} + \dot{V}\right)dt.$$

By (26), the $\mathcal{H}^\infty$ performance level γ is achieved if $\Gamma(k) < 0$, which can be established by,

$$\gamma^{-1}\mathbf{z}^{\mathrm{T}}\mathbf{z} - \gamma\mathbf{d}^{\mathrm{T}}\mathbf{d} + \dot{V} < 0, \tag{27}$$

which is equivalent to the following matrix inequality,

$$\begin{pmatrix} \left(\mathbf{A}+\mathbf{B}_{\mathrm{u}}\mathbf{k}\right)^{\mathrm{T}}\mathbf{P} + \mathbf{P}\left(\mathbf{A}+\mathbf{B}_{\mathrm{u}}\mathbf{k}\right) & (*)^{\mathrm{T}} & (*)^{\mathrm{T}} \\ \mathbf{B}_{\mathrm{d}}^{\mathrm{T}}\mathbf{P} & -\gamma\mathbf{I} & (*)^{\mathrm{T}} \\ \left(\mathbf{C}_z+\mathbf{D}_{\mathrm{u}}\mathbf{k}\right) & \mathbf{D}_{\mathrm{d}} & -\gamma\mathbf{I} \end{pmatrix} < 0 \tag{28}$$

By pre- and post-multiplying, diag$(\mathbf{Q,I,I})$, (28) can be represented as the following LMI constraint in terms of the synthesis variables, $\mathbf{g} := \mathbf{kQ},\ \mathbf{Q} > 0$,

$$\mathcal{L}_{\mathrm{hinf}} := \begin{pmatrix} \mathbf{Q}\mathbf{A}^{\mathrm{T}} + \mathbf{g}^{\mathrm{T}}\mathbf{B}_{\mathrm{u}}^{\mathrm{T}} + \mathbf{A}\mathbf{Q} + \mathbf{B}_{\mathrm{u}}\mathbf{g} & (*)^{\mathrm{T}} & (*)^{\mathrm{T}} \\ \mathbf{B}_{\mathrm{d}}^{\mathrm{T}} & -\gamma\mathbf{I} & (*)^{\mathrm{T}} \\ \mathbf{C}_z\mathbf{Q} + \mathbf{D}_{\mathrm{u}}\mathbf{g} & \mathbf{D}_{\mathrm{d}} & -\gamma\mathbf{I} \end{pmatrix} < 0 \tag{29}$$

4 Design Results

4.1 Controller Construction

The motor electrical control torque τ_{b} in (11) composed of the velocity-dependent control torque $\tau_{\mathrm{b,e}}$ in (10) equilibrium operation and the deviation control torque $\tau_{\mathrm{b,c}}$ to achieve the addressed multi-objective performance as discussed in Section 3.2 to 3.4 and specified by the LMI conditions (22), (25), and (29). The controller synthesis structure is shown in Fig. 2.

In the regulated output constraint via (25), the magnitude bound on the electrical control torque is chosen as, $z_2 = \tau_{\mathrm{b,c}} \le \tau_{\mathrm{b,max}} = \tau_{\mathrm{b,rate}} = 0.6998 := z_{2,\max}$. For the $\mathcal{H}^\infty$ performance specified by (29), two performance levels are considered, one is from the disturbance to the tracking error,

$$\gamma_1 : \mathbf{d}_1 = \begin{pmatrix} \delta\tau_{\mathrm{m}} & \delta\tau_{\mathrm{r}} & r\delta W_\alpha \end{pmatrix}^{\mathrm{T}} \to z_1 = z_{\mathrm{e}},$$

and another is from the tracking command to the control torque, $\gamma_2 : d_2 = v_{\mathrm{d}} \to z_2 = z_{\mathrm{u}}$.

Under the LMIs conditions for invariant set (22) and regulated output (25), if only the γ_1 is considered, the optimal performance level via (29) is $\gamma_1 = 186.7754$. On the other hand, if only the γ_2 performance is optimized, the achieved performance is $\gamma_2 = 277.8316$. For the various $\mathcal{H}^\infty$ performance levels considered for the control torque $\gamma_2 = \{100, 300, 500, 1000\}$, the achieved performance levels on γ_1 are obtained as $\gamma_1 = \{280.4476, 280.0226, 278.5707, 277.9726\}$, using the LMI synthesis tool [15]. The design results are depicted in Fig. 3.

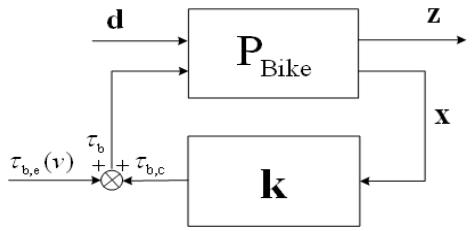

Fig. 2 Framework of optimal controller synthesis

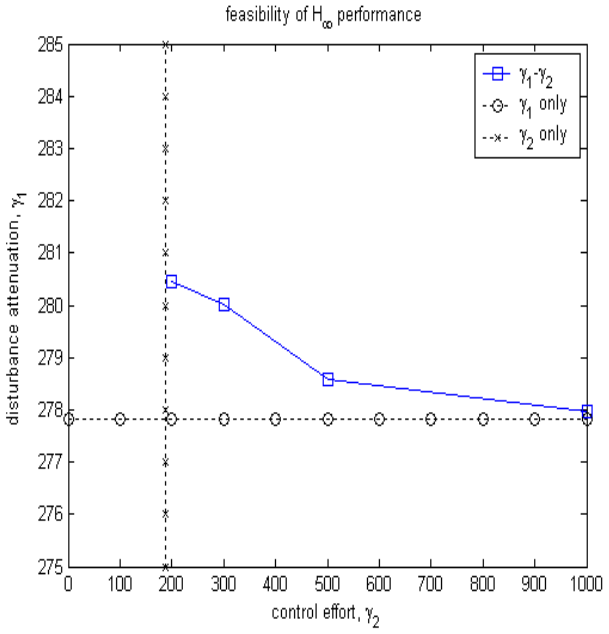

Fig. 3 Optimization of tracking performance under control effort constraint

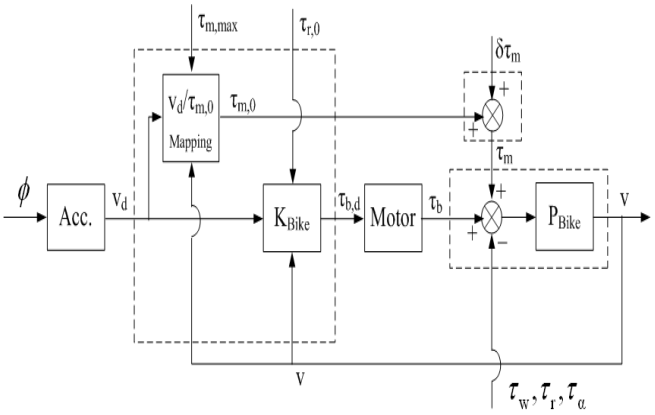

Fig. 4 The system structure for controller simulation

4.2 Time Response Simulation

The system structure for simulation is shown in Fig. 4. In the time-response simulation, the E-Bike is driven by the human torque τ_m, motor electric torque τ_e, and the various resistance torque $\tau_{res} = \tau_w + \tau_r + \tau_\alpha$. The likely human torque in the E-Bike postulated from the mapping by the "$v_d/\tau_{m,d}$ mapping" device in Figure 4 and described by,

$$\tau_{m,d} = \tau_{m,max} \cos\left(\frac{v\pi}{2v_d}\right) \tag{30}$$

where $\tau_{m,max}$ is the available maximum human torque, designated as $\tau_{m,max} = 12\tau_{b,max}$. Also, as shown in Fig. 4, the actual human torque τ_m imposed on the E-Bike is the postulated human torque $\tau_{m,d}$ plus the magnitude and band limited uncertainty on human torque denoted by $\Delta\tau_m$, that is, $\tau_m = \tau_{m,d} + \Delta\tau_m$. In the block denoted by "Acc.", the angle of the accelerator ϕ determines the desired velocity v_d and can be implemented simply as $v_d = \phi v_{max}/\phi_{max}$.

Fig. 5 shows that the external inputs of the E-Bike comprise of the angle of the accelerator ϕ, which represents the desired velocity, and the actual human torque τ_m, which represents the energy added to the E-Bike from the driver. The dynamics of the E-Bike are influenced by its own velocity, including the wind resistance and tire resistance as mentioned in section 2.

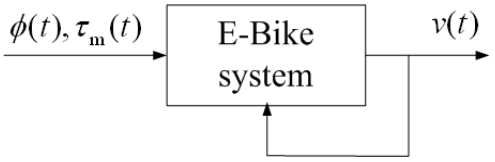

Fig. 5 The input-output schematics of the E-Bike

The various resistances are composed of the wind resistance, rolling resistance, and gradient resistance, and are described by (4), (8), and (9), respectively. The motor electrical torque τ_b in (11) is composed of the velocity-dependent torque $\tau_{b,e}$ from (10) for vehicle equilibratory operation, and the deviated torque $\tau_{b,c}$ from optimization of γ_1 performance while subject to the γ_2 performance constraint via (29), as well as conditions for the state variable invariant set (22) and the regulated output magnitude constraint (25).

In the time-response simulation, the optimal control signal is obtained from optimization of

tracking error performance $\gamma_1 = 278.5707$ while subject to the control torque magnitude performance constraint $\gamma_2 = 500$ from (29). The state-feedback control law is,

$$\mathbf{k} = \begin{bmatrix} -1.9495 & 0.1518 \end{bmatrix}. \qquad (31)$$

The vehicle weight is assumed to be $W = W_{\text{med}} = 80$ (Kg). The tracking command is represented by a low-passed version of step desired velocity $v_{\text{d}} = 5$ (Km/hr), issued in 10 sec from standstill, $v = 0$ (Km/hr).

Two scenarios of time-response simulation are conducted. In one scene of simulation, a flat road condition is considered, with the gradient angle identically zero, $\alpha = 0$. In the second simulation, the road condition is assumed with linear varying gradient angle in time period during 20~40 seconds. Figs. 6 and 7 show the time responses for these two simulations, including the responses of velocity command, actual velocity, motor torque, human torque, and the various resistance torques. As shown, the time-response performance is satisfactory in overall. The feasibility and effectiveness of the controller design methodology proposed in this work for the E-Bike systems is verified.

5 Conclusion

This paper is on the velocity-dependent torque control approach for the light electric bike with human power assistance. The designed velocity control signal includes two parts. One is the velocity-dependent equilibratory torque for compensation of wind resistance. Another is an additional deviation torque to achieve multi-objective performances regarding the external disturbance input, control signal magnitude, and velocity tracking error. The investigated objective-performance includes the invariant set of state variable under the magnitude bounded disturbance, the magnitude bound on the regulated output, and the $\mathcal{H}^{\infty}$ performance optimization for attenuation of disturbance effect on regulated output. Following modeling the electrical bike and introducing specifications of the termed EL-168 electric bike produced by KENTFA Advanced Technology, Taiwan, the design method proposed in this paper was verified through time-response simulations for both the flat and linear varying gradient road conditions.

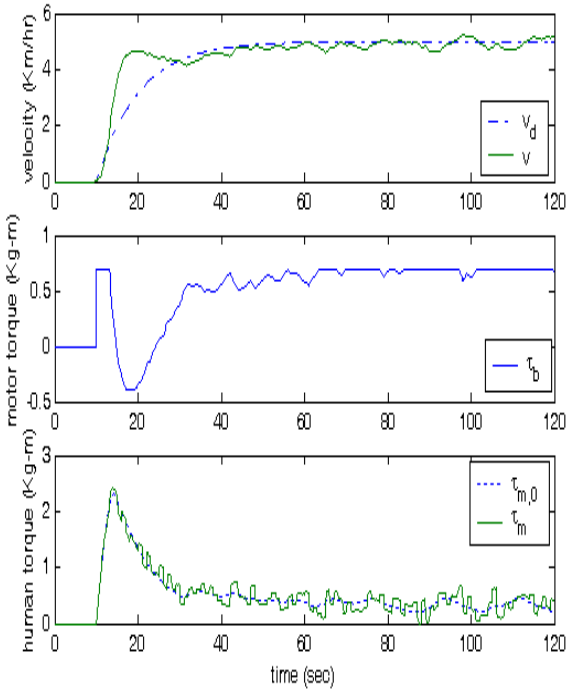

(a)

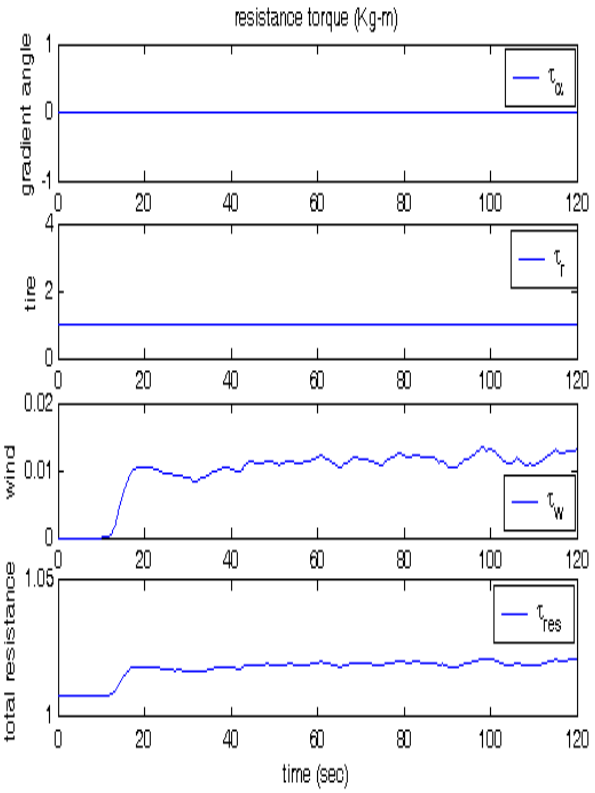

(b)

Fig. 6 Time response of electrical bike under a flat road condition

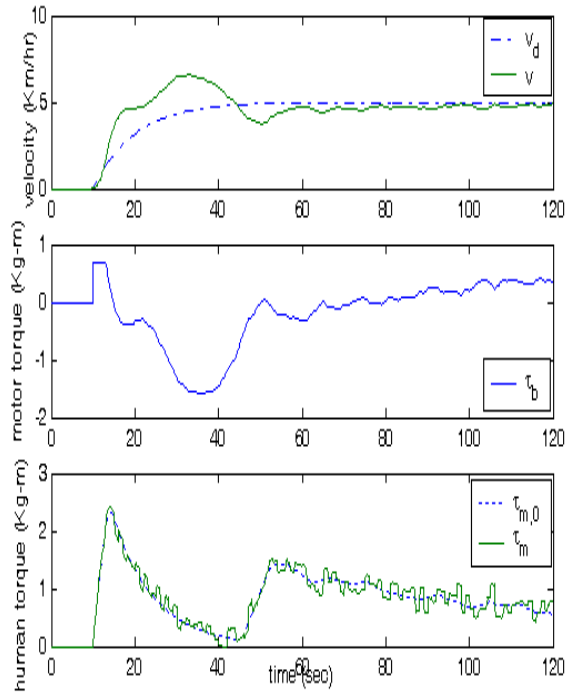

(a)

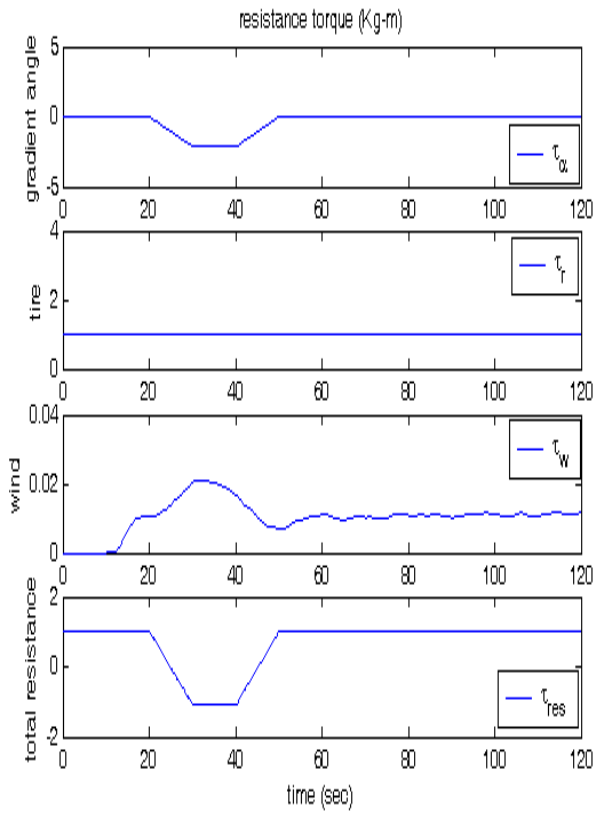

(b)

Fig. 7 Time response of electric bike under a linear varying gradient angle

Nomenclature

A: the vehicle fontal area, $A = 0.35\,(\mathrm{m}^2)$.

C_w: the wind resistance coefficient, $C_w = 1.8$.

F_w: the wind resistance force.

$f_{r,t}, \tau_{r,t}$: the torque friction coefficient, the torque resistance of tire.

$f_{r,c}, \tau_{r,c}$: the contact friction coefficient, the contact resistance of tire.

f_r, τ_r: the total friction coefficient, the total resistance of tire.

g: the gravitational acceleration, $g = 9.8\,(\mathrm{m/sec}^2)$

I: the total moment of inertia of wheel, $I = 0.9\,(\mathrm{Kg\text{-}m}^2)$.

k_p: the proportional gain of torque control, $k_p = 5$.

P_r: the tire pressure, $P_r = 60\mathrm{psi} = 4.22 \times 10^4\,(\mathrm{Kg/m}^2)$.

r_e, r: the rolling, the nominal radius of tire, $r_e \cong r = 12" \times 2.54 / 2 = 0.1524\,(\mathrm{m})$.

r_r: the reaction rolling radius of tire.

v, v_d: the actual, the desired velocity of vehicle.

W: the vehicle weight, including E-Bike and rider.

W_z: the reaction force in the rolling tire.

w_r: the tire width, . $w_r = 1.75\mathrm{in} = 0.044\mathrm{m}$

α, F_α: the angle, the resistance force of gradient.

γ: the air density, $\gamma = 1.293\ (\mathrm{Kg/m}^3)$.

$\tau_b, \tau_{b,d}, \tau_{b,\max}$: the actual, the desired motor torque, $\tau_{b,\max} = 6.8580\,(\mathrm{Nt\text{-}m})$.

$\tau_m, \tau_{m,d}, \Delta\tau_m, \tau_{m,\max}$: the actual, the postulated, the deviated, the maximum of human torque.

$\tau_r, \tau_w, \tau_\alpha$: the tire rolling resistance torque, wind resistance torque, and gradient resistance torque.

θ, ω: the angle, the angular velocity of wheel.

ϕ, $\phi_{\max}$: the actual, the maximum of accelerator angle.

References:

[1] Asian Development Bank, *Electric Bikes in the People's Republic of China: Impact on the Environment and Prospects for Growth, Mandaluyong City*, Philippines,2009.

[2] Astrom, K.J., Klein, R.E., and Lennartsson, A., Bicycle Dynamics and Control, *IEEE Control Systems Magazine*, 2005 , pp. 26–47.

[3] Limebeer, D.J.N. and Sharp, R.S., Single-Track Vehicle Modeling and Control: Bicycles, Motorcycles, and Models, *IEEE Control Systems Magazine*, 2006, pp. 34–61.

[4] Sharp, R.S., On the Stability and Control of the Bicycle, *Transactions of the ASME: Applied Mechanics Reviews,* Vol. 61, 2008, pp. 1–24.
[5] Tanaka, T. and Murakami, T., A Study on Straight-Line Tracking and Posture Control in Electric Bicycle, *IEEE Trans. Industrial Electronics*, Vol. 56, 2009, pp. 159–168.
[6] Hwang, C.L., Wu, H.M. and Shih, C.L., Fuzzy Sliding-Mode Underactuated Control for Autonomous Dynamic Balance of an Electrical Bicycle, *IEEE Trans. Control Systems Technology*, Vol. 17, 2009, pp. 658–670.
[7] Chen, P.H., Intelligent application: ELEBIKE Fuzzy Control: Part 1, *In Proceedings of the Seventh International Conference Machine Learning and Cybernetics*, Kunming, China, 2008, pp. 3581–3585.
[8] Indulal, S. and Nair, P.S.C., A Novel Approach in Automatic Control of a Hybrid Bicycle, *In Proceedings of the IET-UK International Conference on Information and Communication Technology in Electrical Sciences*, Tamil Nadu, India, 2007, pp. 296-301.
[9] Liang, C.-Y., Lin, W.-H., and Chang, B., Applying Fuzzy Control to an Electric Bicycle, *In Proceedings of First International Conference on Innovative Computing, Information and Control*, Beijing, China, 2006, pp.513-516.
[10] Niki, H., Miyata, J., and Murakami, T., Power Assist Control of Electric Bicycle Taking Environment and Rider's Condition into Account, *In Proceedings of the international Society for Optical Engineering,* Sappora, Japan, 2005, 60520H.
[11] Fan, X., Iwase, M., and Tomizuka, M., Non-Uniform Velocity Profile Compensation for an Electric Bicycle Based on Repetitive Control with Sinusoidal and Non-Sinusoidal Internal Models, *In Proceedings of the ASME Dynamic systems and Control Conference*, Hollywood CA, USA, 2010, pp. 765-772.
[12] Zhou, H., Long, B., and Cao, B.G., $\mathcal{H}^{\infty}$ Robust Controller for Electric Bicycles, *In Proceedings of Workshop on Power Electronics and Intelligent Transportation System*, Guangzhou, China, 2008, pp. 131-135.
[13] Hong, B.S., Lin, T.Y., and Su, W.J., LPV Modeling and Synthesis for Energy-Efficient E-Eilks, *In Proceedings of 2009 CACS International Automatic Control Conference*, Taipei, Taiwan, 2009.
[14] Boyd, S., Ghaoui, L.El., Feron, E., and Balakrishnan, V., *Linear Matrix Inequalities in System and Control Theory*, SIAM, Philadelphia, 1994.
[15] Gahinet, P., Nemirovski, A., Laub, A. and Chilali, M., *The LMI Control Toolbox*, The MathWorks, MA, 1994.